Journal of Petroleum Research and Studies

journal homepage: https://jprs.gov.iq/index.php/jprs/

Print ISSN 2220-5381, Online ISSN 2710-1096

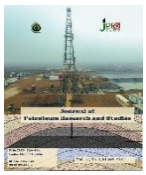

Thermodynamic Modeling of Wax Deposition Phase Behavior for Reservoir Fluid in Southern Iraqi Oil Field

Mohammed A. Ahmed, Ali A. Rashak*, Mohammed E. Resan

Oil and Gas Engineering Department, University of Technology, Baghdad, Iraq

*Corresponding Author E-mail: ali.amjed.rashak@gmail.com

Article Info

Received 30/09/2024
Revised 06/04/2025
Accepted 09/04/2025
Published 19/03/2026

DOI:
http://doi.org/10.52716/jprs.v16i1.1023

Abstract

Most reservoir fluids contain heavy paraffinic compounds that may precipitate as a solid or solid-like material called wax if the fluid is cooled down. Wax precipitation may cause operational problems when unprocessed well streams are transported in undersea pipelines, in which the temperature may fall to that of the surrounding seawater. Wax may deposit as a solid layer inside the pipeline. With continued transport, this layer will build up and eventually plug the pipeline if not mechanically removed. The need to proactively predict the temperature at which wax will precipitate leads to the development and application of thermodynamic models for such prediction. This study aims to develop a thermodynamic model to predict the wax deposition envelope (WDE), which gives a good idea of the temperature at which wax precipitation occurs. Using a live oil sample from southern Iraqi oilfield, this study used the Soave-Redlich-Kwong (SRK-EOS) model that can predict the specific conditions at which wax precipitation occurs as well as respond to the reservoir fluid. The SRK-EOS results in the Multiflash program were matched with the fluid and wax experimental data. The results pointed out that wax precipitation would happen in tandem with the same production scenario after the temperature dropped.

Keywords: Wax deposition, Thermodynamic modeling, Phase behavior, Flow assurance.

نموذج ثرموديناميكي لسلوك طور ترسب الشمع لسائل مكمني في حقل نفط جنوب العراق

الخلاصة

تحتوي معظم سوائل المكمن على مركبات بارافينية ثقيلة قد تترسب على شكل مادة صلبة أو شبيهة بالصلبة تسمى الشمع إذا تم تبريد السائل. قد يتسبب ترسب الشمع في حدوث مشاكل تشغيلية عندما يتم نقل الموائع المنتجة من اللآبار غير المعالجة في خطوط الأنابيب تحت سطح البحر، حيث قد تنخفض درجة الحرارة إلى درجة حرارة مياه البحر المحيطة. قد يترسب الشمع على شكل طبقة صلبة داخل خط الأنابيب. مع استمرار النقل، ستتراكم هذه الطبقة وتسد خط الأنابيب في النهاية إذا لم تتم إزالتها ميكانيكيًا. تؤدي الحاجة إلى التنبؤ بشكل استباقي بدرجة الحرارة التي سيترسب عندها الشمع إلى تطوير وتطبيق نماذج ثرموديناميكية لمثل هذا التنبؤ. تهدف هذه الدراسة إلى تطوير نموذج ثرموديناميكي للتنبؤ بمخطط ترسب الشمع (WDE)، والذي يعطي فكرة جيدة عن درجة الحرارة التي يحدث عندها ترسب الشمع. بأستخدام

عينة نفط حية من حقل نفطي في جنوب العراق، استخدمت هذه الدراسة نموذج Soave-Redlich-Kwong (SRK-EOS) الذي يمكنه التنبؤ بالظروف المحددة التي يحدث عندها ترسب الشمع بالإضافة إلى الأستجابة لسائل المكمن. تمت مطابقة نتائج SRK-EOS في برنامج Multiflash مع البيانات التجريبية للسائل والشمع. وأشارت النتائج إلى أن ترسب الشمع سيحدث بالتزامن مع نفس سيناريو الإنتاج بعد إنخفاض درجة الحرارة.

1. Introduction

Wax deposition is a major flow assurance problem in the oil industry, restricting crude oil flow in pipelines, causing pressure abnormalities, and potentially leading to reduced production or abandonment of facilities in severe cases. It also results in formation damage near the wellbore, reduced permeability, and changes in fluid properties such as increased viscosity and gelation due to phase separation as solid wax precipitates [1]. The deposit is not solid wax but a gel comprising solid wax crystals and trapped liquid, which hardens over time through a process known as aging. Wax primarily consists of high molecular weight n-paraffins with long-chain alkanes (20 to 50 carbon atoms) that precipitate when the oil temperature drops below the wax appearance temperature (WAT), the point at which the first wax crystals form during cooling [2]. Wax precipitation is particularly problematic in low-temperature environments like deep offshore fields and fields after the temperature decline, where deposits may also contain asphaltenes, resins, and fines [3]. Several methods have been presented to the industry for coping with wax-related problems. These methods fall into three different categories; thermal, mechanical, and chemical. All these methods have their disadvantages in that they increase operating expenses. Therefore, it is essential to be able to predict the amount and conditions of wax precipitation to reduce operating expenses [4].

1.1. Area of Study

The area of study is Southern Iraqi Oilfield - Nahr Umr Formation, as shown in Figure (1). The Oilfield, located southeast of Iraq, spans 30 km by 10 km. It contains significant oil reserves in the Nahr Umr Formation, a key sandstone reservoir with medium porosity and high permeability. This formation consists of sandstone and mud shale, deposited in a tide-controlled, marine-continental transitional environment. [5].

Fig. (Error! No text of specified style in document.**): Location of Oilfield.**

2. Materials and Data

This study predicted wax precipitation under both ambient surface and reservoir conditions using reservoir and experimental data. The modeling simulation relied on compositional characterization and fluid dynamics data from experiments. It focused on a crude oil sample from wells in the Oilfield. Details of the data used are provided in later sections.

2.1. Well data: Table (1) shows the fundamental information of the reservoir and the well.

Table (1): Reservoir and Well Data.

Field	X
Reservoir fluid	Oil
Reservoir pressure, psi	5056 psig
Reservoir temperature, Fº	243 Fº
Oil API	27.1
Wellhead Pressure	893 psig
Wellhead Temperature	91 Fº
Choke size	12/64
Sample	BHS (live oil)
Sampling depth	3500 m

2.2. Compositional Analysis of Reservoir Fluid:

Compositional analysis uses gas chromatography (GC) to measure hydrocarbons and components in oil and gas samples. Gas compositions are analyzed for hydrocarbons from C_1 to C_{15}^+ and other gases, while liquid samples are analyzed up to C_{36}^+ using specialized methods. [6,7].

Table (2) shows plus-fraction properties, while Table (3) lists the compositional analysis of the reservoir fluid sample up to C_{36}^{+}.

Table (2): Plus-fraction Data.

	Calculated properties	Flashed Liquid	Flashed Gas	Recombined Fluid
C_7	Mole%	90.23	2.68	45.7
	Molecular Weight (g / mol)	298.8	101.9	292.9
	Density at 60°F (g / cm^3)	0.9079	0.7246	0.9056
C_{36}	Mole%	10.7		5.27
	Molecular Weight (g / mol)	988.1		988.1
	Density at 60°F (g / cm^3)	1.0673		1.0673

Table (2): Compositional Analysis of the Reservoir Fluid Sample Up to 36+

	Component	Flashed Liquid Mole %	Flashed Gas Mole %	Recombined Fluid Mole %
H_2	Hydrogen	0	0	0
H_2S	Hydrogen Sulphide	0	0	0
CO_2	Carbon Dioxide	0	1.99	1.01
N_2	Nitrogen	0	0.45	0.23
C_1	Methane	0.03	52.77	26.84
C_2	Ethane	0.18	14.06	7.24
C_3	Propane	0.62	11.21	6.01
iC_4	i-Butane	0.28	2.18	1.25
nC_4	n-Butane	1.21	5.9	3.6
C_5	Neo-Pentane	0	0.01	0.01
iC_5	i-Pentane	1.09	2.53	1.82
nC_5	n-Pentane	1.84	3.09	2.48
C_6	C6 Hexanes	4.52	3.13	3.81
C_7	M-C-Pentane	0.79	0.32	0.55
	Benzene	0.15	0.05	0.1
	Cyclohexane	0.38	0.25	0.31
	Heptanes	5.21	1.02	3.08
C_8	M-C-Hexane	0.93	0.15	0.53
	Toluene	0.6	0.07	0.33
	Octanes	6.03	0.51	3.22
C_9	E-Benzene	0.45	0.01	0.23
	M/P-Xylene	0.98	0.05	0.51
	O-Xylene	0.41	0.01	0.2

	Nonanes	5.33	0.16	2.7
C_{10}	1,2,4-TMB	0.5	0	0.24
	Decanes	5.96	0.05	2.95
C_{11}	Undecanes	5.71	0.03	2.82
C_{12}	Dodecanes	4.91	0	2.41
C_{13}	Tridecanes	4.51	0	2.22
C_{14}	Tetradecanes	3.77	0	1.85
C_{15}	Pentadecanes	3.6	0	1.77
C_{16}	Hexadecanes	3.17	0	1.56
C_{17}	Heptadecanes	2.68	0	1.32
C_{18}	Octadecanes	2.53	0	1.24
C_{19}	Nonadecanes	2.44	0	1.2
C_{20}	Eicosanes	2.11	0	1.04
C_{21}	Heneicosanes	1.87	0	0.92
C_{22}	Docosanes	1.68	0	0.83
C_{23}	Tricosanes	1.52	0	0.75
C_{24}	Tetracosanes	1.39	0	0.68
C_{25}	Pentacosanes	1.25	0	0.61
C_{26}	Hexacosanes	1.13	0	0.56
C_{27}	Heptacosanes	1.04	0	0.51
C_{28}	Octacosanes	0.99	0	0.49
C_{29}	Nonacosanes	0.95	0	0.46
C_{30}	Triacontanes	0.9	0	0.44
C_{31}	Hentriacontanes	0.87	0	0.43
C_{32}	Dotriacontanes	0.78	0	0.38
C_{33}	Tritriacontanes	0.72	0	0.35
C_{34}	Tetratriacontanes	0.7	0	0.35
C_{35}	Pentatriacontanes	0.59	0	0.29
C_{36}^{+}	Hexatriacontanes plus	10.7	0	5.27
	Total	100%	100%	100%

2.3. Experimental data of PVT properties

Several investigations were conducted to establish the characteristics of the oil post retrieving a sample of crude oil from the bottom hole under reservoir conditions (known as live oil) from a one well [8]. The outcomes of each experiment were explained as mentioned below.

2.3.1. The Constant Mass Expansion (CME) or Constant Composition Expansion (CCE):

Table (3): Constant Composition Expansion (CCE) at 243 F.

Pressure (psig)	Liquid density (g/cm3)	relative volume =V/Vsat	Y function	compressibility (psi ^-6) *10^-6
8000	0.7948	0.9492		0.00000601
7502	0.7924	0.9521		0.00000628
7010	0.7899	0.9551		0.00000657
6506	0.7872	0.9584		0.00000689
6011	0.7844	0.9617		0.00000724
5514	0.7816	0.9653		0.00000763
5488	0.7814	0.9655		0.00000765
Pres= 5056	0.7788	0.9687		0.00000803
5007	0.7784	0.9691		0.00000807
4510	0.7752	0.9731		0.00000856
4010	0.7718	0.9774		0.0000091
3508	0.7686	0.9821		0.00000973
3011	0.7644	0.987		0.00001044
2515	0.7603	0.9923		0.00001125
2006	0.7557	0.9982		0.00001215
1972	0.7554	0.9987		0.0000122
1961	0.7553	0.9988		0.00001222
1933	0.7551	0.9991		0.00001225
1909	0.7548	0.9994		0.00001227
1883	0.7546	0.9998		0.00001227
Pb= 1863	0.7544	1		
1859		1.0007	3.076	
1853		1.0017	3.072	
1847		1.0028	3.068	
1836		1.0048	3.06	
1823		1.0072	3.052	
1796		1.0122	3.034	
1743		1.0227	2.999	
1649		1.0438	2.937	
1497		1.0853	2.835	
1276		1.1692	2.686	
1001		1.3401	2.497	
833		1.5109	2.38	
670		1.7702	2.264	
564		2.0265	2.188	
488		2.2825	2.133	
415		2.622	2.079	
361		2.9572	2.04	
321		3.2886	2.009	
281		3.7036	1.979	

2.3.2. Differential Vaporization (DLE):

Table (4): Differential Vaporization (DLE) at 243 F.

Pressure (psig)	RS (scf/bbl)	Bod (relative oil volume	Btd(relative total volume)	oil density (g/cm3)	Z	Bg ft3/scf	gas gravity
1863	465	1.356	1.356	0.7544			
1600	415	1.334	1.434	0.7609	0.913	0.0113	0.76
1350	368	1.312	1.545	0.7676	0.919	0.0134	0.769
1100	320	1.289	1.719	0.7746	0.927	0.0166	0.787
850	272	1.267	2.01	0.7812	0.937	0.0216	0.811
600	223	1.243	2.571	0.7893	0.949	0.0307	0.855
350	170	1.216	3.987	0.7978	0.964	0.0526	0.954
100	91	1.173	12.583	0.8073	0.984	0.1709	1.326
0	0	1.085		0.8328			2.212

2.3.3.Viscosity:

Table (5): Reservoir Fluid Viscosity Data at 243 F.

pressure (psig)	oil viscosity (cp)	calculated gas viscosity (cp)
8000	1.805	
7500	1.75	
7000	1.695	
6500	1.64	
6000	1.585	
5500	1.531	
5056	1.482	
5000	1.476	
4500	1.421	
4000	1.366	
3500	1.311	
3000	1.257	
2500	1.202	
2000	1.147	
1863	1.132	
1600	1.224	0.0164
1350	1.297	0.0158
1100	1.359	0.0152
850	1.421	0.0146
600	1.504	0.0139
350	1.674	0.0131
100	2.256	0.0114
0	4.252	

2.3.4. SARA Fraction:

Table (6): SARA Fraction %.

Saturate hydrocarbon	63.23 wt %
Aromatic	24.36 wt %
Resin	5.11 wt%
Asphaltene	7.3%
Hydrocarbons Ratio (Saturates/Aromatics)	2.6
Non- Hydrocarbons Ratio (Resins/Asphaltenes)	0.7

2.4. Methodology and Equations

2.4.1. Wax Precipitation Modeling Using Multiflash Software

The PVT report of a well in the target field contains crucial data for this model, including reservoir data such as temperature and local pressure, fluid properties such as GOR and Pb, reservoir fluid composition analyses. To create a model of wax precipitation, all of this data was inputted into the Multiflash software, and the SRK-EOS equation of state was used to calculate wax precipitation modeling. Figure (2) depicts the block diagram of Wax phase envelope (WPE) modeling.

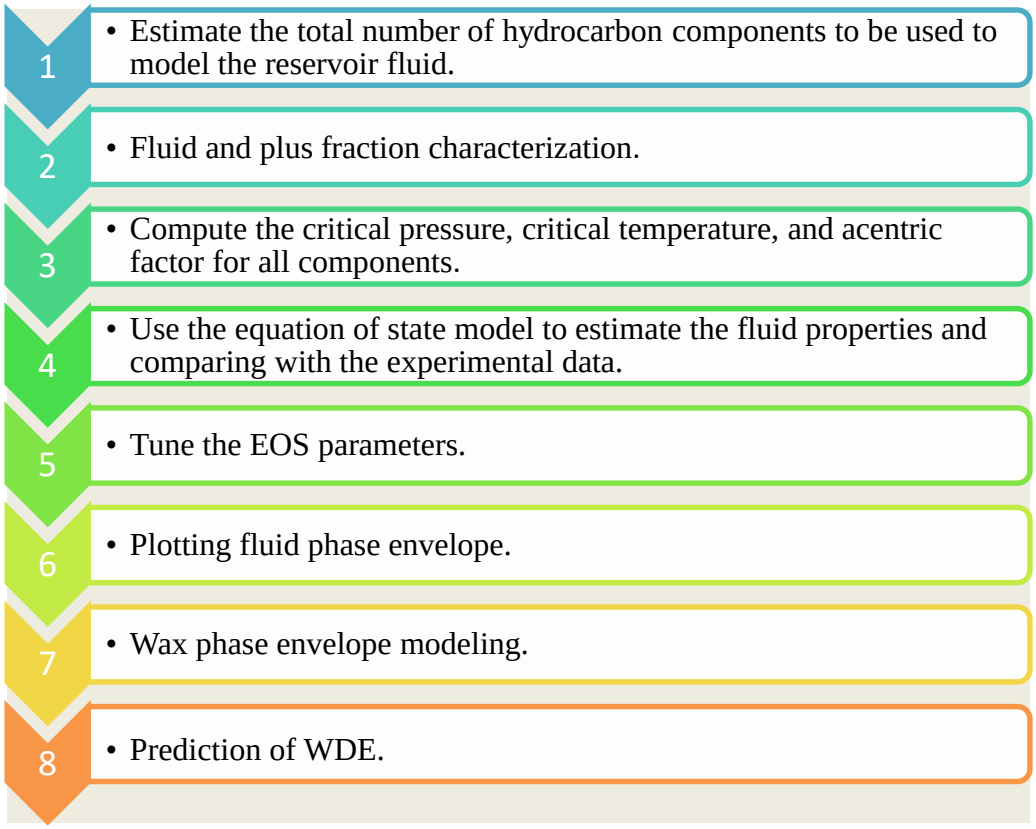

Fig. (2): Fluid and Wax Modeling Methodology.

2.4.2. Soave-Redlich-Kwong Equation of State (SRK)

The Soave-Redlich-Kwong (SRK) equation of state is a widely used thermodynamic model for calculating the properties of fluids, particularly gases and liquids. It was developed by R. C. Reid, J. M. Prausnitz, and B. E. Poling in 1971, based on modifications to the original Redlich-Kwong (RK) equation proposed by O. Redlich and J. N. S. Kwong in 1949 [9].

The SRK equation incorporates corrections to the RK equation to better account for molecular interactions and non-ideal behavior, particularly in systems with moderate to high pressures [10]. The equation is expressed as:

$$p = \frac{RT}{v-b} - \frac{a}{v(v+b)} \quad \text{..... (1)}$$

Where a and b are the EOS model parameters. The pure component parameters (a and b) can be calculated by:

$$a = \Omega_a \frac{R^2 T_c^2}{p_c} \alpha(T) \quad \text{..... (2)}$$

$$b = \Omega_b \frac{RT_c}{p_c} \quad \text{..... (3)}$$

$$\alpha(T) = \left[1 + m(\omega)\left(1 - \sqrt{\frac{T}{T_c}}\right)\right]^2 \quad \text{..... (4)}$$

In equations 2, 3, and 4 the coefficients $\Omega_a = 0.42748$ and $\Omega_b = 0.08664$, and the value of $\alpha(T)$ can be calculated by:

$$m(\omega) = 0.480 + 1.574\omega - 0.176\omega^2 \quad \text{..... (5)}$$

Where P is the pressure, *T* is the temperature, *V* is the molar volume, *R* is the ideal gas constant, a and b are constants related to the molecular properties of the substance, the critical pressure (p_c), critical temperature (T_c), acentric factor (ω) and molecular weight (MW).

3. Result and Discussion

3.1. Fluid Characterization

Crude oil is a complex mixture containing thousands of unique molecules. Analyzing each one individually is impractical for reservoir fluid modeling. Instead, engineers employ a process called characterization to represent the oil with a manageable number of simplified components.

Beginning with C_{36}, the C_{36}^+ fraction is divided into 10 pseudo-components. The distribution of single carbon numbers (SCN) is one approach used in oil modeling, with Pedersen correlation and

laboratory testing used to tune the results. This will provide us a more detailed fraction distribution than the lab report. Figure (3) shows the match between the observed and calculated SCN.

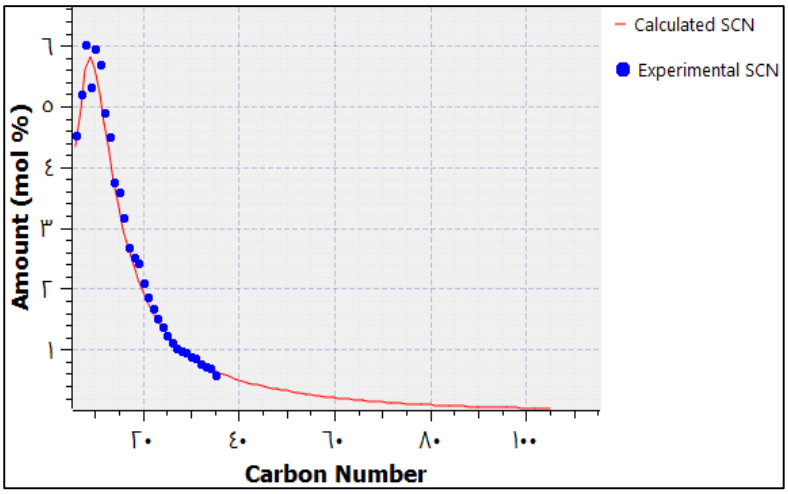

Fig. (3): The Left-Skewed and Exponential Distribution.

3.2. Matching (Tuning) of Fluid Model with PVT Experiments

Matching involves adjusting an EOS model's simulation data to align with experimental data for a specific reservoir fluid. Since phase behavior models based on the fluid's EOS can be inaccurate, adjustments are made. Live oil, consisting of many components, is simplified into carbon groups and pure substances through splitting and lumping. To reduce discrepancies between estimated and actual values, various input data in the phase behavior model are modified [14].

3.3. Matching Results

In the following section, we will delve into the specific matching outcomes of each property that resulted from the trial-and-error approach we previously implemented. The details of these outcomes are presented below:

- In Figure (4) displays the matching of Pb at different temperatures. As observed from the graph, the experimental values of Pb correspond well with the values calculated by the SRK-model.

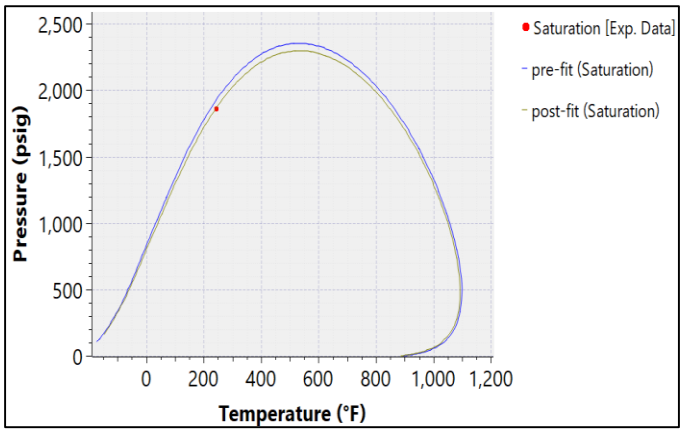

Fig. (4): Bubble Point Matching.

- Differential Liberation Tests: Figures (5) to (10) showcase the comparison of differential liberation tests for Bo, Rs, Bg, ρo, Z-factor, and gas gravity. The simulated data generated by the SRK-model aligns well with the experimental data, indicating a strong agreement between the two.

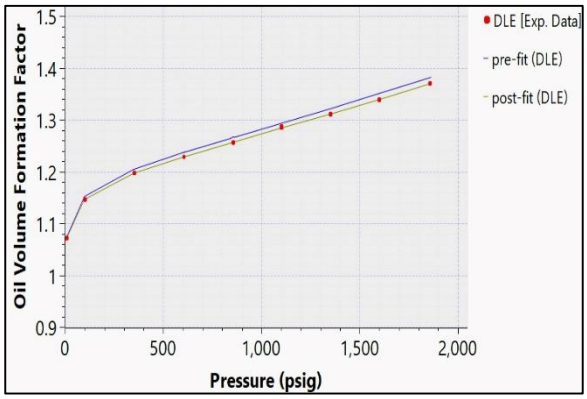

Fig. (5): Oil Formation Volume Factor Matching.

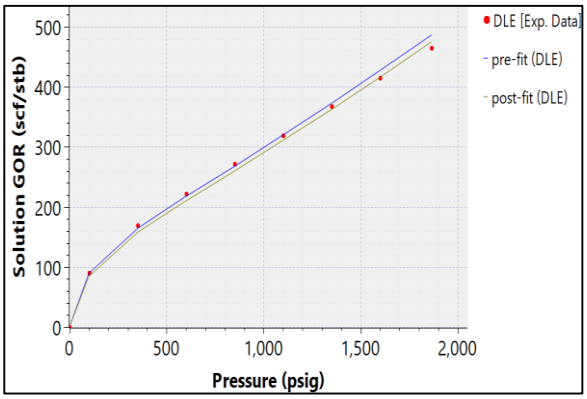

Fig. (6): Solution Gas-Oil Ratio Matching.

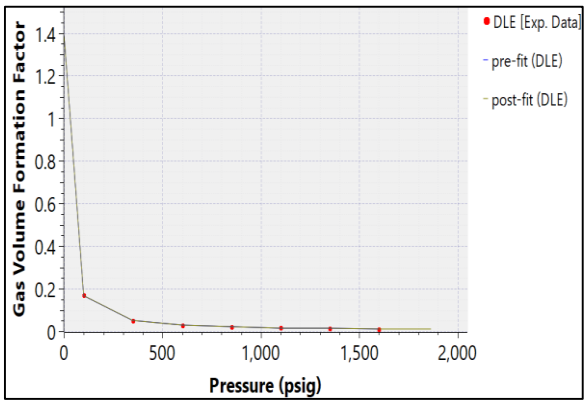

Fig. (7): Gas Volume Formation Factor Matching.

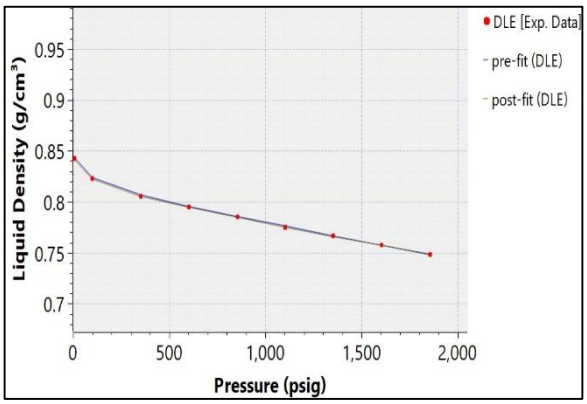

Fig. (8): Liquid Density Matching.

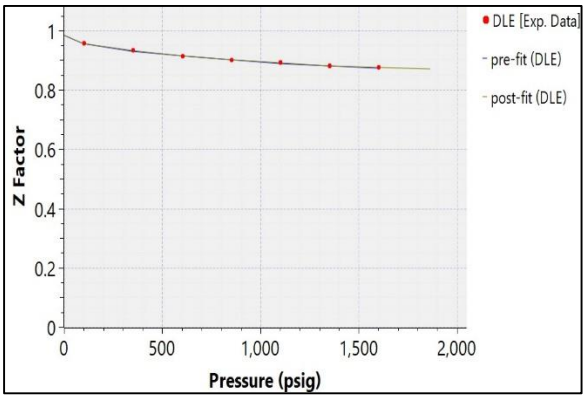

Fig. (9): Z Factor Matching.

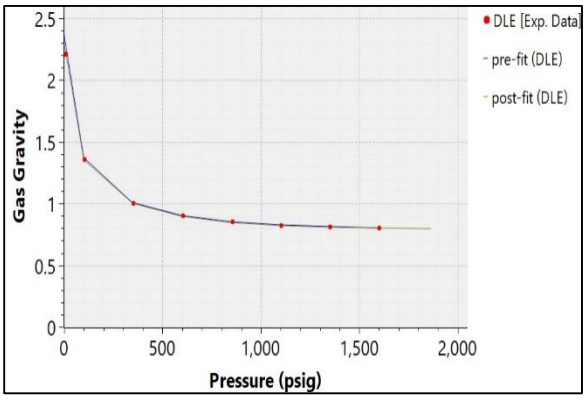

Fig. (10): Gas Gravity Matching.

- Figures (11), (12) illustrates the comparison of flash liberation tests such as liquid density and relative volume for constant composition expansion experiments. The simulated data and experimental data exhibit a high degree of agreement, indicating that the simulation accurately represents the experimental conditions.

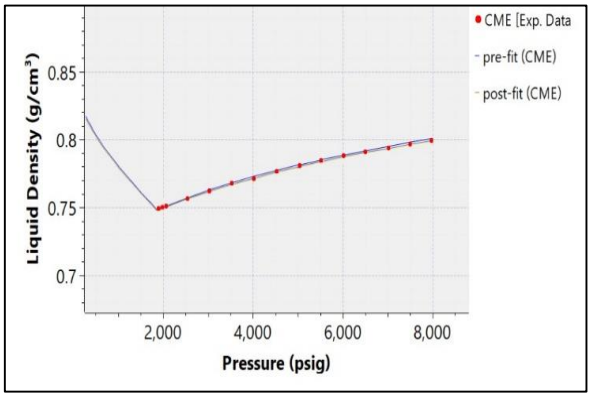

Fig. (11): Liquid Density Matching.

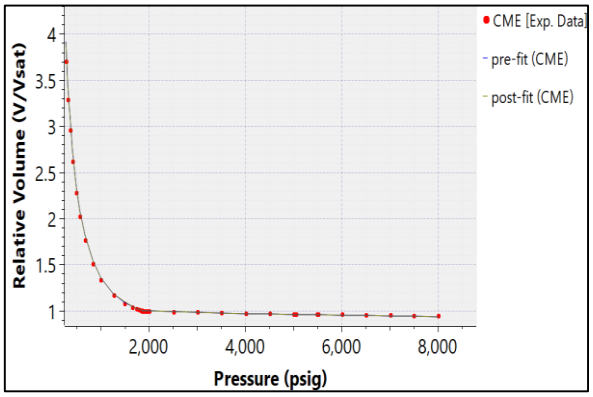

Fig. (12): Relative Volume Matching.

- In the field of Oil and Gas Viscosity Measurement Tests, the viscosity calculations in Multiflash software are based on the corresponding state principle. These calculations are defined by the form suggested by Pedersen et al. The default viscosity tuning is set accordingly.

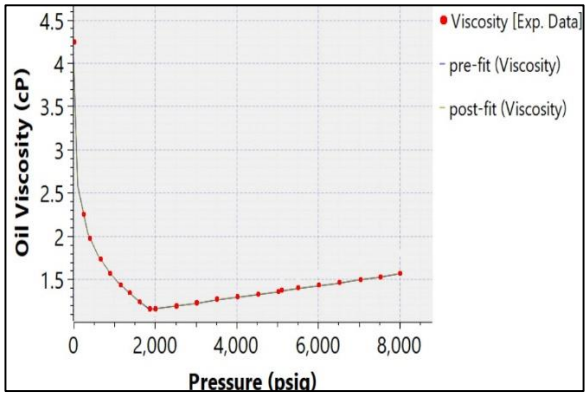

Fig. (13): Oil Viscosity Matching.

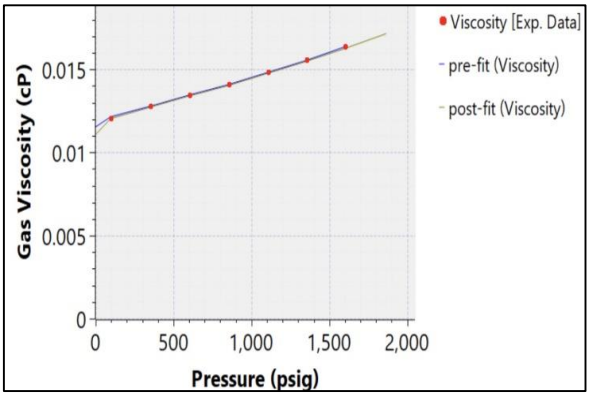

Fig. (14): Gas Viscosity Matching.

Essentially, the process of tuning leads to a simulation that agrees acceptably with fluid PVT experiments. This allows for the resulting fluid model to be leveraged with confidence in various subsurface and surface facility computations.

3.4. Wax Phase Envelope

The multiflash software utilizes the Soave-Redlich-Kwong (SRK) equation to create the wax phase envelope. In Figure (15), the red line depicts the phase envelope between oil and gas, with the area inside the line indicating a two-phase state and the area outside representing a single phase. The blue vertical line signifies the wax phase envelope, providing insights into the pressure and temperature conditions leading to precipitation. The right side of the line indicates no wax precipitation concerns, while the left side signifies potential wax appearance issues.

Assessing the Oilfield's reservoir conditions reveals that the pressure and temperature values align with the non-wax side, indicating no risk of wax precipitation. However, the wellhead conditions, represented by the green dot, fall on the left side of the wax line, signifying a potential wax precipitation problem. If production continues under these conditions, the wax issue could worsen. Additionally, the flow line, denoted by the pink dot, also lies within the wax region. The green line represents the projected production path under constant production pressure, temperature, and choke sizes.

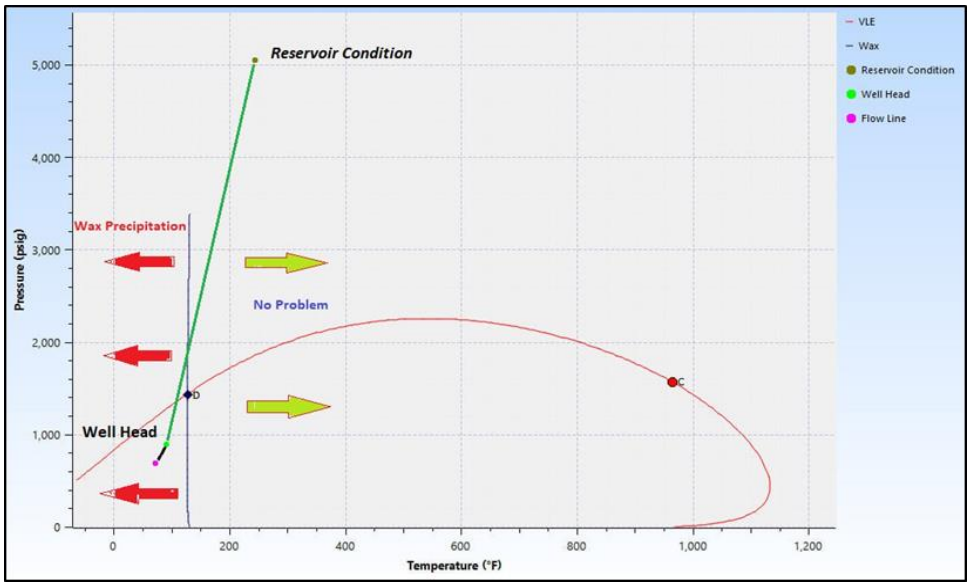

Fig. (15): Phase Envelope of Wax.

The Figure (16) created using multiflash software illustrates the correlation between the changes in pressure and temperature with wax mass percent of liquid. Each colored line in the figure represents a pressure value ranging from 14.7 to 1000, aimed at examining the impact of both pressure and temperature. The analysis indicates that temperature has a substantially greater influence on the wax mass percent of liquid compared to pressure. Despite the significant variation in pressure values, its effect on wax mass percent is relatively minor. This finding aligns with previous research [15, 16] and underscores the dominant role of temperature in this context.

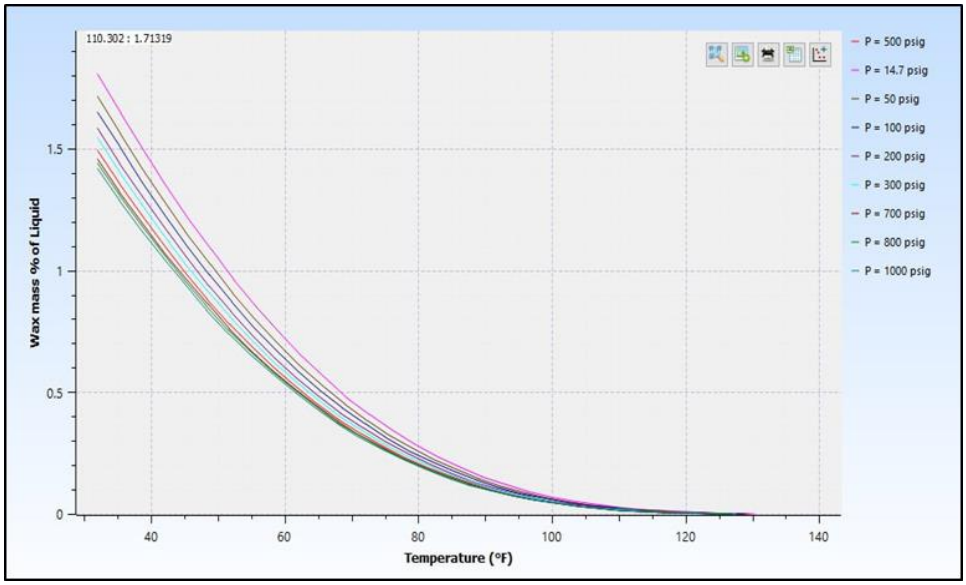

Fig. (16): Relation of Temperature and Wax Mass with Pressure.

4. Conclusion

- **Wax Deposition Risks in the Oilfield:** A phase diagram analysis conducted on a well producing from the Nahr Umr Formation has identified wax deposition as a significant challenge affecting production efficiency. According to the study, wax precipitation begins when the temperature within the production system including the reservoir, wellbore, and surface equipment falls below **130°F (54.44°C)**, increasing the likelihood of flow restrictions and blockages.
- **Operational Impact:** If the temperature drops below **130°F (54.44°C)**, the well may experience partial or complete blockages, leading to production decline, higher maintenance costs, and increased operational interventions. Persistent wax deposition without effective mitigation measures could result in substantial production losses and negatively impact the long-term economic viability of the field.
- **Implications for Other Wells:** Given that production conditions in other wells producing from the same geological formation are likely to be similar, these wells may also be susceptible to wax deposition. Proactive monitoring, thermal management strategies, and chemical or mechanical mitigation techniques should be implemented to prevent flow assurance issues and maintain production efficiency.

Author Contributions Statement: Mohammed A. Ahmed contributed to the Conception; Writing Original Draft. Ali A. Rashak contributed to the Methodology; Experiments; Data Interpretation. Mohammed E. Resan contributed to the Experiments; Writing – Review & Editing. All authors have read and approved the final version of the manuscript.

References

[1] M. A. Theyab, "Wax deposition process: mechanisms, affecting factors and mitigation methods", *Open Access J. Sci*., vol. 2, no. 2, pp. 112-118, 2018. https://doi.org/10.15406/oajs.2018.02.00054.

[2] N. N. Johnson-Achilike, and G. A. Chukwu, and J. Ajienka, "Thermodynamic Modelling for Mapping Wax Deposition Envelope for an Identified Niger Delta Oilfield", presented at *SPE Nigeria Annual International Conference and Exhibition*, Aug. 2015, p. SPE-178317, 2015. https://doi.org/10.2118/178317-MS.

[3] R. C. Albagli, L. B. Souza, and A. O. Nieckele, "Reynolds number influence on wax deposition", presented at *Offshore Technology Conference Brasil*, Oct. 2017, p. D031S025R002, 2017. https://doi.org/10.4043/28053-MS.

[4] J. I. Aguiar, A. A. Nerris, and A. Mahmoudkhani, "Can Paraffin Wax Deposit Above Wax Appearance Temperature? A Detailed Experimental Study", presented at *SPE Annual Technical*

Conference and Exhibition, p. SPE-201297-MS, Oct. 2020. https://doi.org/10.2118/201297-MS.

[5] D. Stratiev, I. Shishkova, R. Nikolova, T. Tsaneva, M. Mitkova, and D. Yordanov, "Investigation on precision of determination of SARA analysis of vacuum residual oils from different origin", *Petroleum & Coal*, vol. 58, no. 1, pp. 109-119, 2016.

[6] P. Ilushin, K. Vyatkin, and A. Kozlov, "Development of a New Model for the Formation of Wax Deposits through the Passage of Crude Oil within the Well", *Sustainability*, vol. 15, no. 12, p. 9616, 2023. https://doi.org/10.3390/su15129616.

[7] F. O. Ochieng, M. N. Kinyanjui, J. O. Abonyo, and P. R. Kiogora, "Mathematical Modeling of Wax Deposition in Field-Scale Crude Oil Pipeline Systems", *Journal of Applied Mathematics*, 2022. https://doi.org/10.1155/2022/2845221.

[8] O. M. Akinyede, "Development of a Thermodynamic Model for Wax Precipitation in Produced Crude Oil—Case Study of Hydrocarbon Fluid from Niger-Delta, Nigeria", *Ph.D. dissertation, African University of Science and Technology*, Abuja, Nigeria, 2019.

[9] A. A. Olajire, "Review of wax deposition in subsea oil pipeline systems and mitigation technologies in the petroleum industry", *Chemical Engineering Journal Advances*, vol. 6, p. 100104, 2021. https://doi.org/10.1016/j.ceja.2021.100104.

[10] J. Wang, F. Zhou, L. Zhang, Y. Huang, E. Yao, L. Zhang, F. Wang, and F. Fan, "Experimental study of wax deposition pattern concerning deep condensate gas in Bozi block of Tarim Oilfield and its application", *Thermochimica Acta*, vol. 671, pp. 1-9, 2019. https://doi.org/10.1016/j.tca.2018.10.024.

[11] M. K. Rogachev, T. N. Van, and A. N. Aleksandrov, "Technology for preventing the wax deposit formation in gas-lift wells at offshore oil and gas fields in Vietnam", *Energies*, vol. 14, no. 16, p. 5016, 2021. https://doi.org/10.3390/en14165016.

[12] J. H. Gary, J. H. Handwerk, and M. J. Kaiser, "Petroleum Refining: Technology and Economics", 5th ed., *CRC Press*, 2007. https://doi.org/10.4324/9780203907924.

[13] M. A. Ahmed, G. H. Abdul-Majeed, and A. K. Alhuraishawy, "Modeling of asphaltene precipitation using CPA-EOS for live oil in an Iraqi oil well", in *AIP Conference Proceedings*, vol. 2839, no. 1, p. 020038, AIP Publishing LLC, 2023. https://doi.org/10.1063/5.0167684.

[14] S. M. H. Hashemi, K. Monfaredi, and B. Sedaee, "An inclusive consistency check procedure for quality control methods of the black oil laboratory data", *Journal of Petroleum Exploration and Production Technology*, vol. 10, pp. 2153-2173, 2020. https://doi.org/10.1007/s13202-020-00869-6

[15] S. Rezaee, "Separation and Characterization of Crude Oils and Investigation of Their Wetting Properties on Rock Surfaces", *Ph.D. dissertation, Rice University*, 2019.

[16] H. Yin, Y. Chen, X. You, Z. Chen, D. He, and H. Gong, "SARA Characterization and Comparison for the Ultra-Heavy Oil via Combined Analyses", *Journal of Energy Resources Technology*, vol. 145, no. 11, 2023. https://doi.org/10.1115/1.4062925.